Hindawi Publishing Corporation
Advances in High Energy Physics
Volume 2015, Article ID 197930, 16 pages
http://dx.doi.org/10.1155/2015/197930

Review Article

A Review on ϕ Meson Production in Heavy-Ion Collision

Md. Nasim,[1] Vipul Bairathi,[2] Mukesh Kumar Sharma,[3] Bedangadas Mohanty,[2] and Anju Bhasin[3]

[1] *Department of Physics and Astronomy, UCLA, Los Angeles, CA 90095, USA*
[2] *School of Physical Sciences, National Institute of Science Education and Research, Bhubaneswar 751005, India*
[3] *Physics Department, University of Jammu, Jammu 180001, India*

Correspondence should be addressed to Bedangadas Mohanty; bedanga@niser.ac.in

Received 29 July 2014; Accepted 2 October 2014

Academic Editor: Fu-Hu Liu

The main aim of the relativistic heavy-ion experiment is to create extremely hot and dense matter and study the QCD phase structure. With this motivation, experimental program started in the early 1990s at the Brookhaven Alternating Gradient Synchrotron (AGS) and the CERN Super Proton Synchrotron (SPS) followed by Relativistic Heavy Ion Collider (RHIC) at Brookhaven and recently at Large Hadron Collider (LHC) at CERN. These experiments allowed us to study the QCD matter from center-of-mass energies ($\sqrt{s_{NN}}$) 4.75 GeV to 2.76 TeV. The ϕ meson, due to its unique properties, is considered as a good probe to study the QCD matter created in relativistic collisions. In this paper we present a review on the measurements of ϕ meson production in heavy-ion experiments. Mainly, we discuss the energy dependence of ϕ meson invariant yield and the production mechanism, strangeness enhancement, parton energy loss, and partonic collectivity in nucleus-nucleus collisions. Effect of later stage hadronic rescattering on elliptic flow (v_2) of proton is also discussed relative to corresponding effect on ϕ meson v_2.

1. Introduction

According to quantum chromodynamics (QCD) [1–4], at very high temperature (T) and/or at high density, a deconfined phase of quarks and gluons is expected to be present, while at low T and low density the quarks and gluons are known to be confined inside hadrons. The heavy-ion collisions (A + A) provide a unique opportunity to study QCD matter in the laboratory experiments. The medium created in the heavy-ion collision is very hot and dense and also extremely short-lived (~5–10 fm/c). In experiments, we are only able to detect the freely streaming final state particles emerging from the collisions. Using the information carried by these particles as probes, we try to understand the properties of the medium created in the collision.

The ϕ vector meson, which is the lightest bound state of s and $\bar{s}$ quarks, is considered as a good probe for the study of QCD matter formed in heavy-ion collisions. It was discovered at Brookhaven National Laboratory in 1962 through the reaction $K + p \rightarrow \Lambda + K + \overline{K}$ as shown in Figure 1 [5]. It has a mass of 1.019445 ± 0.000020 GeV/c^2 which is comparable to the masses of the lightest baryons such as proton (0.938 GeV/c^2) and Λ (1.115 GeV/c^2). The interaction cross-section (σ) of the ϕ meson with nonstrange hadrons is expected to have a small value [6]. The data on coherent ϕ photo-production shows that $\sigma_{\phi N} \sim 10$ mb [7]. This is about a factor of 3 times lower than $\sigma_{\rho N}$ and $\sigma_{\pi N}$, about a factor of 4 times lower than $\sigma_{\Lambda N}$ and σ_{NN}, and about a factor of 2 times lower than σ_{KN}. Therefore its production is expected to be less affected by the later stage hadronic interactions in the evolution of the system formed in heavy-ion collisions. A hydrodynamical inspired study of transverse momentum (p_T) distribution of ϕ meson seems to suggest that it freezes out early compared to other hadrons [8]. The life time of the ϕ meson is ~42 fm/c. Because of longer life time the ϕ meson will mostly decay outside the fireball and therefore its daughters will not have much time to rescatter in the hadronic phase. Therefore, properties of ϕ meson are primarily controlled by the conditions in the early partonic phase and those can be considered as a clean probe

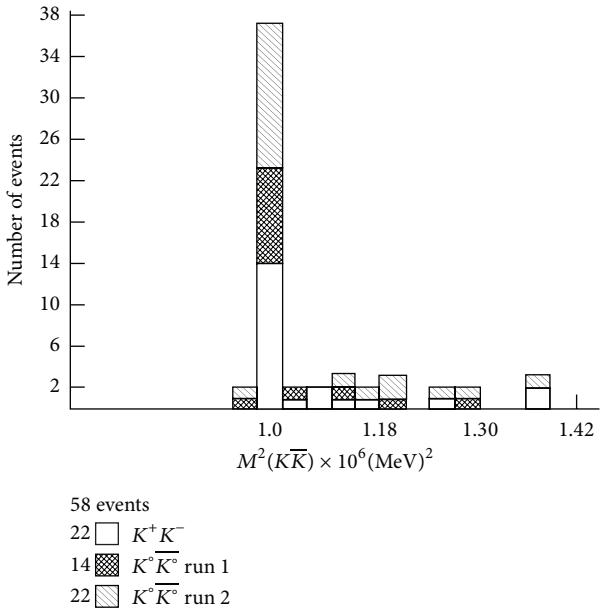

FIGURE 1: Number of events versus square of invariant mass of $K\overline{K}$ pairs from the reaction $K + p \rightarrow \Lambda + K + \overline{K}$ in bubble chamber experiments at Brookhaven National Laboratory (BNL) [5].

to investigate the properties of matter created in heavy-ion collisions.

Strange particle production is one of the observables that is expected to deliver detailed information on the reaction dynamics of relativistic nucleus-nucleus collisions [9]. In experiments at the CERN SPS accelerator it was found that the ratio of the number of produced kaons to that of pions is higher by a factor of about two compared to that in proton-proton reactions at the same energy [10–13]. In the past, several possible reasons for this strangeness enhancement have been discussed. Firstly, if nucleus-nucleus reactions proceed through a deconfined stage, then strange-quark production should be enhanced relative to a no QGP scenario [14]. Alternative ideas of Canonical suppression of strangeness in small systems (proton-proton) as a source of strangeness enhancement in high energy nucleus-nucleus collisions have been proposed [15]. This led to a lot of ambiguity in understanding the true physical origin of the observed enhancement in the strange particle production in high energy heavy-ion collisions. The $\phi(s\bar{s})$ meson due to its zero net strangeness is not subjected to Canonical suppression effects. Therefore measurement of ϕ meson yield in both nucleus-nucleus and proton-proton would provide the true answer for observed strangeness enhancement.

Experimentally measured results on v_2 ($= \langle \cos 2(\varphi - \Psi) \rangle$, a measure of the azimuthal angle (φ) anisotropy of the produced particles, and Ψ is the reaction plane angle) of identified hadrons as a function of p_T show that at low p_T (<2 GeV/c) elliptic flow follows a pattern ordered by mass of the hadron (the v_2 values are smaller for heavier hadrons than that of lighter hadrons). At the intermediate p_T (2 GeV/c to 6 GeV/c) all mesons and all baryons form two different groups [35]. When v_2 and p_T are scaled by the number of constituent quarks (n_q) of the hadrons, the magnitude of the scaled v_2 is observed to be the same for all the hadrons at the intermediate p_T. This observation is known as number-of-constituent quark scaling (NCQ scaling). This effect has been interpreted as collectivity being developed at the partonic stage of the evolution of the system in heavy-ion collision [36, 37]. Since ϕ meson has mass (1.0194 GeV/c^2) comparable to the masses of the lightest baryons such as proton and at the same time it is a meson, the study of ϕ meson v_2 would be more appropriate to understand the mass type and/or particle type (baryon-meson) dependence of $v_2(p_T)$.

In this review we have compiled all the available experimental measurements on ϕ meson production in high energy heavy-ion collisions as a function of p_T, azimuthal angle (φ), and rapidity (y). This paper is organised in the following manner. In Section 2, measurement of ϕ meson invariant yield has been presented from SPS to LHC energy. Section 3 describes the compilation of the azimuthal anisotropy measurements in ϕ meson production from all the available experimental results. Finally, the summary and conclusion have been discussed in Section 4.

2. Invariant Yield of ϕ Meson

2.1. Invariant Transverse Momentum Spectra. We have compiled the data on the invariant p_T spectra of the ϕ meson measured in $p + p$, d + A, and A + A systems for different collision centralities at various centre-of-mass energies ($\sqrt{s_{NN}}$ = 17.3 GeV–7 TeV) [16–22] and those are shown in Figure 2. Only the statistical errors are indicated as error bars. Measurement of ϕ meson invariant yield in $p + p$ collisions at $\sqrt{s} = 7$ TeV by the ATLAS collaboration [38] is consistent with that from the ALICE experiment and hence is not shown in Figure 2. The dashed black lines in Figure 2 are fits to the experimental data using an exponential function of the form

$$\frac{1}{2\pi p_T}\frac{d^2N}{dydp_T} = \frac{dN/dy}{2\pi T\left(m_0 + T\right)}\exp\left[-\frac{\sqrt{m_0^2 + p_T^2} - m_0}{T}\right]. \quad (1)$$

The blue solid lines in Figure 2 are the fits to the data with Levy function of the form given by

$$\frac{1}{2\pi p_T}\frac{d^2N}{dydp_T} = \frac{dN}{dy}\frac{(n-1)(n-2)}{2\pi nT\left(nT + m_0(n-2)\right)} \times\left(1 + \frac{\sqrt{p_T^2 + m_0^2} - m_0}{nT}\right)^{-n}. \quad (2)$$

T is known as the inverse slope parameter, dN/dy is the ϕ meson yield per unit rapidity, m_0 is the rest mass of ϕ meson, and n is the Levy function parameter. Levy function is similar in shape to an exponential function at low p_T and has a power-law-like shape at higher p_T. In fact, the exponential function is the limit of the Levy function as n approaches infinity. From Figure 2, it can be seen that the exponential

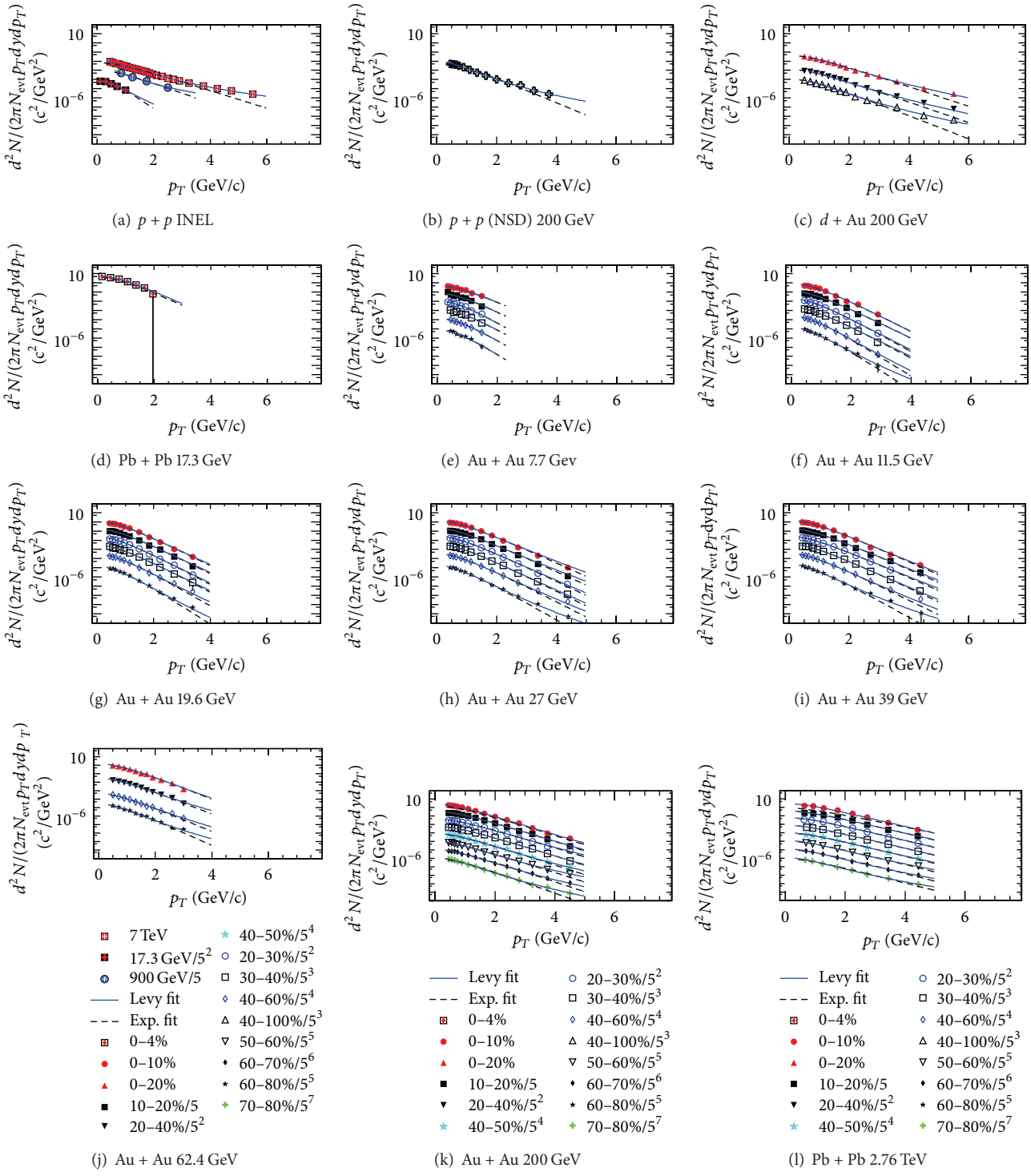

FIGURE 2: The invariant yield of ϕ mesons as a function of p_T measured for different system and different centralities at various centre-of-mass energies [16–21]. The black dashed (blue solid) line represents an exponential (Levy) function fit to the data.

and Levy functions both fit the central collision data equally well. However, with decreasing centrality, the exponential fits diverge from the data at higher transverse momentum and the Levy function fits the data better. The χ^2/ndf values are larger for exponential function fits in peripheral collisions compared to Levy function fits (see Tables 1 and 2). This indicates a change in shape of the p_T spectra (deviations from exponential distribution and more towards a power law distribution) at high p_T for peripheral collisions. Tsallis function also describes the measured identified spectra

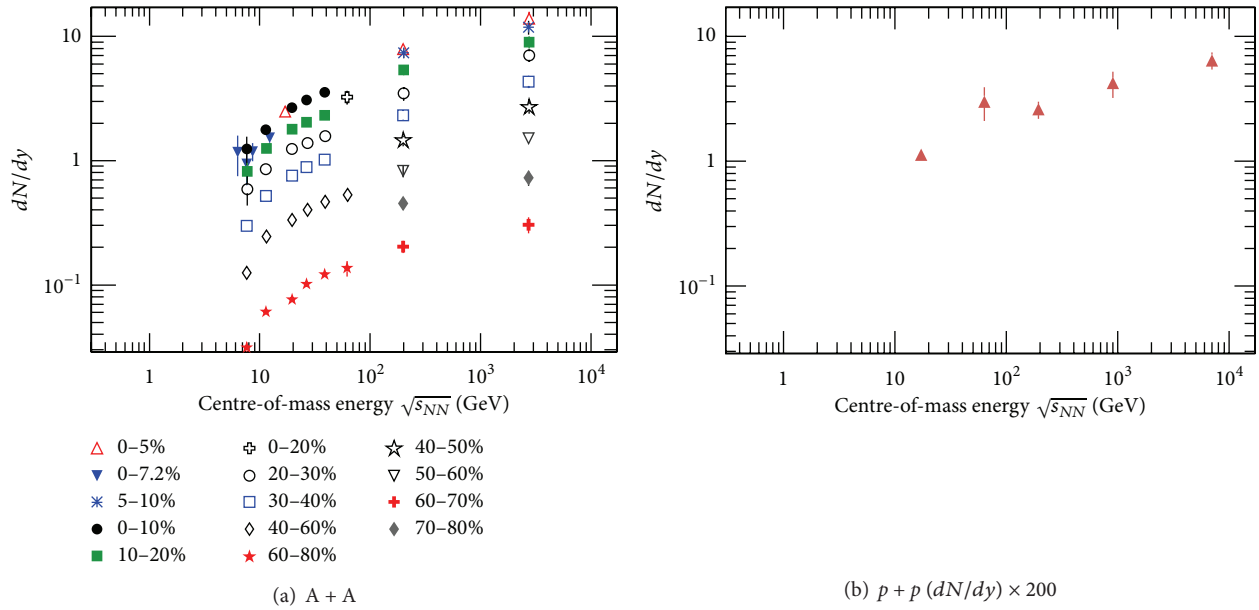

(a) A + A

(b) $p + p$ (dN/dy) × 200

FIGURE 3: The ϕ meson midrapidity yield (dN/dy) as a function of $\sqrt{s_{NN}}$ for A + A [16–18, 21] and $p + p$ collisions [18–20, 22, 23]. For RHIC BES energies ($\sqrt{s_{NN}}$ = 7.7–39 GeV) only statistical errors are shown whereas for other energies systematic errors are added in quadrature with statistical errors.

equally well as Levy, which is shown in [39, 40]. Like Levy, Tsallis function describes both the low p_T exponential and the high p_T power law behaviors. The Tsallis function has two parameters while number of parameters for Levy is three. The exponential function fails to explain data at high p_T for $p + p$ and d + Au collisions whereas Levy function describes data for all p_T. This evolution in the shape of the spectra from exponential-like in central collisions to more power-law-like in peripheral collisions reflects the increasing contribution from pQCD (hard) processes to ϕ meson production in more peripheral collisions at higher p_T. Particle production at low p_T is expected to be due to nonperturbative soft processes and with sufficient interactions the system could be thermalized, and that is why both exponential and Levy functions fit the data for all centralities at low p_T. All the Levy and exponential fit parameters for A + A collisions are given in Tables 1 and 2. One can see that the values of parameter n are large in the case central A + A collisions where both Levy and exponential functions fit the data well. The dN/dy values increase from peripheral to central collisions, indicating increasing production of ϕ meson with increase in collision centrality.

2.2. ϕ Meson Yield per Unit Rapidity. In Figure 3 we present all available measurements of p_T integrated ϕ meson yield (dN/dy) at midrapidity as a function of centre-of-mass energy in both nucleus-nucleus [16–18, 21] and proton-proton collisions [18–20, 22, 23]. For A + A collisions, different centralities are shown by different marker styles in Figure 3(a). The measured midrapidity yield increases with centrality and for the same centrality it increases with the collision energy for both A + A and $p + p$ collisions. The rate of increases with $\sqrt{s_{NN}}$ is higher in A + A collisions compared to $p + p$ collisions. We have observed that the measured midrapidity yield per participant (N_{part}) pair, $(dN/dy)/(0.5N_{\text{part}})$, increases nonlinearly with centrality and for the same $N_{\text{part}}(dN/dy)/(0.5N_{\text{part}})$ increases with the collision energy of the A + A collisions. The former suggests that particle production does not scale with N_{part} and the latter is expected because of the increase of energy available to produce the ϕ mesons.

2.3. Strangeness Enhancement. The ratio of strange hadron production normalised to $\langle N_{\text{part}}\rangle$ in nucleus-nucleus collisions relative to corresponding results from $p+p$ collisions at 200 GeV [24] is shown in the left upper panel of Figure 4. The results are plotted as a function of $\langle N_{\text{part}}\rangle$. K^-, Λ, and Ξ are found to exhibit an enhancement (value > 1) that increases with the number of strange valence quarks. Furthermore, the observed enhancement in these open-strange hadrons increases with collision centrality, reaching a maximum for the most central collisions. However, the enhancement of ϕ meson production from Cu + Cu and Au + Au collisions shows a deviation in ordering in terms of the number of strange constituent quarks. Such deviation is also observed in central Pb + Pb collisions at SPS energy (as shown in the right bottom panel of Figure 4). The difference in the ordering does not seem to be a baryon-meson effect, since K^- and Λ have similar enhancement, or a mass effect, since Λ and ϕ have similar mass but different enhancement factors.

In heavy-ion collisions, the production of ϕ mesons is not Canonically suppressed due to its $s\bar{s}$ structure. The $p + p$ collisions at RHIC are at an energy which is ~25 times higher than energies where violations of the Okubo-Zweig-Iizuka (OZI) rule were reported [41, 42]. The observed enhancement of ϕ meson production then is a clear indication for the

Table 1: Results from Levy fits to the transverse mass distributions of the ϕ meson. All values are for midrapidity ($|y| < 0.5$).

	Centrality	χ^2/ndf	T (GeV)	n	dN/dy
Pb + Pb (2.76 TeV)	0–10%	4.282/5	0.5005 ± 0.0128	$1.121e^{06}$ ± $1.414e^{06}$	12.41 ± 0.796
	10–20%	4.793/5	0.5131 ± 0.0132	$4.969e^{05}$ ± $2.6e^{05}$	8.978 ± 0.553
	20–30%	3.976/5	0.4926 ± 0.0429	162 ± 681.2	6.870 ± 0.415
	30–40%	1.796/5	0.4897 ± 0.0454	129.6 ± 436.7	4.190 ± 0.262
	40–50%	2.25/5	0.4401 ± 0.0424	28.34 ± 21	2.605 ± 0.162
	50–60%	3.177/5	0.3946 ± 0.042	15.41 ± 6.68	1.457 ± 0.094
	60–70%	0.551/5	0.3801 ± 0.0432	14.68 ± 6.23	0.7157 ± 0.050
	70–80%	0.910/5	0.3401 ± 0.04351	10.41 ± 3.32	0.297 ± 0.022
Au + Au (200 GeV)	0–10%	9.4/11	0.3572 ± 0.002331	102.9 ± 116	7.421 ± 0.106
	10–20%	19.2/11	0.3529 ± 0.002514	93.2 ± 101	5.142 ± 0.108
	20–30%	15.2/11	0.3591 ± 0.002343	41.6 ± 5.6	3.442 ± 0.071
	30–40%	16.2/11	0.3595 ± 0.002448	38.9 ± 20	2.189 ± 0.045
	40–50%	21.4/11	0.3153 ± 0.003802	22.7 ± 4.3	1.392 ± 0.033
	50–60%	6.9/11	0.2905 ± 0.003404	0.0138 ± 1.9	0.806 ± 0.023
	60–70%	7.4/11	0.2916 ± 0.002911	0.0186 ± 3.6	0.419 ± 0.014
	70–80%	5.5/11	0.2430 ± 0.002543	0.0130 ± 2.3	0.202 ± 0.009
Au + Au (62.4 GeV)	0–20%	9.2/8	0.3211 ± 0.00624	$9.993e^{06}$ ± $6.39e^{06}$	3.693 ± 0.353
	20–40%	8.8/8	0.3217 ± 0.00353	$4.24e^{08}$ ± $7.41e^{06}$	1.590 ± 0.142
	40–60%	14.5/8	0.2910 ± 0.00644	$9.409e^{07}$ ± e^{10}	0.580 ± 0.071
	60–80%	6.78/6	0.2681 ± 0.001426	21.45 ± 17.89	0.151 ± 0.020
Au + Au (39 GeV)	0–10%	1.645/9	0.2995 ± 0.01611	$6.619e^{10}$ ± $8.931e^{05}$	3.402 ± 0.812
	10–20%	1.046/9	0.3131 ± 0.03514	$1.108e^{07}$ ± $1.414e^{04}$	2.216 ± 0.278
	20–30%	1.55/8	0.2996 ± 0.01301	$1.532e^{08}$ ± $6.651e^{05}$	1.597 ± 0.150
	30–40%	1.047/9	0.2957 ± 0.04906	945 ± 356	1.019 ± 0.0773
	40–60%	1.6383/9	0.2363 ± 0.03561	24.47 ± 14.96	0.456 ± 0.057
	60–80%	1.705/9	0.2110 ± 0.03410	20.2 ± 10.72	0.128 ± 0.018
Au + Au (27 GeV)	0–10%	3.719/9	0.2861 ± 0.007709	89.17 ± 78.22	3.051 ± 0.178
	10–20%	10.05/9	0.2851 ± 0.0039	56.62 ± 38.42	2.004 ± 0.0278
	20–30%	12.85/9	0.2747 ± 0.01754	46.3 ± 32.98	1.345 ± 0.082
	30–40%	14.06/9	0.2574 ± 0.01741	40.36 ± 30.44	0.846 ± 0.053
	40–60%	2.573/9	0.2114 ± 0.01696	19.3 ± 6.155	0.404 ± 0.026
	60–80%	15.946/9	0.1901 ± 0.01368	23.34 ± 7.753	0.107 ± 0.007
Au + Au (19.6 GeV)	0–10%	10.28/8	0.2803 ± 0.00466	87.17 ± 69.63	2.603 ± 0.051
	10–20%	10.96/8	0.2676 ± 0.01202	59.38 ± 47.27	1.786 ± 0.037
	20–30%	9.75/8	0.2367 ± 0.01038	32.32 ± 13.11	1.263 ± 0.029
	30–40%	8.804/8	0.2397 ± 0.01144	33.25 ± 26.33	0.759 ± 0.018
	40–60%	14.31/8	0.1947 ± 0.00865	15.19 ± 2.743	0.336 ± 0.007
	60–80%	7.346/8	0.1913 ± 0.00553	15.76 ± 2.849	0.080 ± 0.001
Pb + Pb (17.3 GeV)	0–4%	1.329/2	0.1746 ± 0.01043	1000 ± $1.175e^{05}$	0.00227 ± 0.0013
Au + Au (11.5 GeV)	0–10%	6.694/7	0.2662 ± 0.009276	100.73 ± 75.39	1.733 ± 0.112
	10–20%	8.171/7	0.2653 ± 0.01187	60.29 ± 42.09	1.121 ± 0.076
	20–30%	4.599/7	0.2282 ± 0.02887	37.3 ± 32.05	0.772 ± 0.054
	30–40%	10.18/7	0.2353 ± 0.03014	34.36 ± 30.39	0.467 ± 0.034
	40–60%	2.898/7	0.1846 ± 0.02255	18.9 ± 10.09	0.205 ± 0.015
	60–80%	1.034/7	0.1438 ± 0.01981	11.31 ± 3.681	0.056 ± 0.005
Au+Au (7.7 GeV)	0–10%	1.5978/4	0.3082 ± 0.03636	90.33 ± 79.97	1.21 ± 0.098
	10–20%	2.8/4	0.2419 ± 0.02615	64.29 ± 40.33	0.719 ± 0.061
	20–30%	2.946/4	0.1639 ± 0.07128	50.19 ± 35.39	0.518 ± 0.091
	30–40%	1.299/4	0.2039 ± 0.02201	63.3 ± 39.39	0.275 ± 0.024
	40–60%	1.833/4	0.1562 ± 0.04774	7.10 ± 6.67	0.139 ± 0.015
	60–80%	2.816/4	0.1423 ± 0.0842	15.02 ± 52.03	0.033 ± 0.007

Table 2: Results from exponential fits to the transverse mass distributions of the ϕ meson. All values are for midrapidity ($|y| < 0.5$).

	Centrality	χ^2/ndf	T (GeV)	dN/dy
Pb + Pb (2.76 TeV)	0–10%	4.28/6	0.5005 ± 0.0128	12.41 ± 0.795
	10–20%	4.793/6	0.5131 ± 0.013	8.973 ± 0.502
	20–30%	4.032/6	0.5024 ± 0.0127	4.032 ± 0.412
	30–40%	1.88/6	0.5027 ± 0.0130	4.171 ± 0.013
	40–50%	4.036/6	0.4961 ± 0.0137	2.550 ± 0.0162
	50–60%	8.356/6	0.4901 ± 0.0146	1.408 ± 0.014
	60–70%	5.937/6	0.4891 ± 0.0156	0.679 ± 0.047
	70–80%	10.12/6	0.4815 ± 0.0182	0.271 ± 0.024
Au + Au (200 GeV)	0–10%	11.2/12	0.3562 ± 0.002431	7.440 ± 0.106
	10–20%	9.7/12	0.3522 ± 0.002614	5.371 ± 0.108
	20–30%	26.7/12	0.3731 ± 0.002413	3.435 ± 0.071
	30–40%	21.1/12	0.3873 ± 0.002548	2.291 ± 0.045
	40–50%	26.4/12	0.3671 ± 0.00307	1.342 ± 0.033
	50–60%	70/12	0.3605 ± 0.003604	0.727 ± 0.023
	60–70%	54.4/12	0.3516 ± 0.003911	0.380 ± 0.014
	70–80%	31.7/12	0.3330 ± 0.004543	0.170 ± 0.009
Au + Au (62.4 GeV)	0–20%	8.4/9	0.328 ± 0.00624	3.523 ± 0.353
	20–40%	8.4/9	0.324 ± 0.00353	1.590 ± 0.140
	40–60%	14.5/9	0.308 ± 0.00644	0.584 ± 0.072
	60–80%	13.3/9	0.2791 ± 0.01426	0.152 ± 0.022
Au + Au (39 GeV)	0–10%	10.36/10	0.3015 ± 0.0052	3.549 ± 0.070
	10–20%	15.54/10	0.3019 ± 0.00522	2.347 ± 0.045
	20–30%	3.946/9	0.3004 ± 0.005711	1.618 ± 0.030
	30–40%	12.57/10	0.2826 ± 0.00398	1.067 ± 0.019
	40–60%	20.62/10	0.267 ± 0.00362	0.498 ± 0.006
	60–80%	21.08/10	0.2371 ± 0.00501	0.124 ± 0.002
Au + Au (27 GeV)	0–10%	26.13/10	0.29 ± 0.00245	3.46 ± 0.036
	10–20%	32.3/10	0.2873 ± 0.00227	2.152 ± 0.023
	20–30%	24.93/10	0.2766 ± 0.00236	1.471 ± 0.016
	30–40%	13.57/10	0.2645 ± 0.00225	0.926 ± 0.010
	40–60%	25.19/10	0.2601 ± 0.00217	0.422 ± 0.004
	60–80%	71.08/10	0.2296 ± 0.00250	0.100 ± 0.001
Au + Au (19.6 GeV)	0–10%	28.87/9	0.2805 ± 0.003265	2.609 ± 0.038
	10–20%	15.28/9	0.2788 ± 0.003722	1.817 ± 0.026
	20–30%	13.63/9	0.2608 ± 0.003246	1.187 ± 0.017
	30–40%	7.811/9	0.2652 ± 0.003917	0.763 ± 0.011
	40–60%	17.78/9	0.2404 ± 0.003352	0.345 ± 0.004
	60–80%	10.06/9	0.2142 ± 0.003558	0.072 ± 0.001
Pb + Pb (17.3 GeV)	0–4%	1.337/3	0.1748 ± 0.01043	0.0022 ± 0.0012
Au + Au (11.5 GeV)	0–10%	11.5/8	0.2621 ± 0.006674	1.754 ± 0.047
	10–20%	9.638/8	0.265 ± 0.006731	1.281 ± 0.033
	20–30%	6.885/8	0.2359 ± 0.006009	0.843 ± 0.022
	30–40%	1.946/8	0.2453 ± 0.005765	0.506 ± 0.013
	40–60%	2.862/8	0.2071 ± 0.00545	0.235 ± 0.005
	60–80%	11.12/8	0.1947 ± 0.00888	0.051 ± 0.001
Au + Au (7.7 GeV)	0–10%	3.36/5	0.3082 ± 0.03087	1.207 ± 0.069
	10–20%	10.46/5	0.2553 ± 0.01811	0.783 ± 0.036
	20–30%	9.767/5	0.2207 ± 0.0141	0.471 ± 0.023
	30–40%	4.177/5	0.2375 ± 0.01926	0.329 ± 0.017
	40–60%	0.4763/5	0.2195 ± 0.01467	0.147 ± 0.007
	60–80%	3.958/5	0.1992 ± 0.02282	0.035 ± 0.002

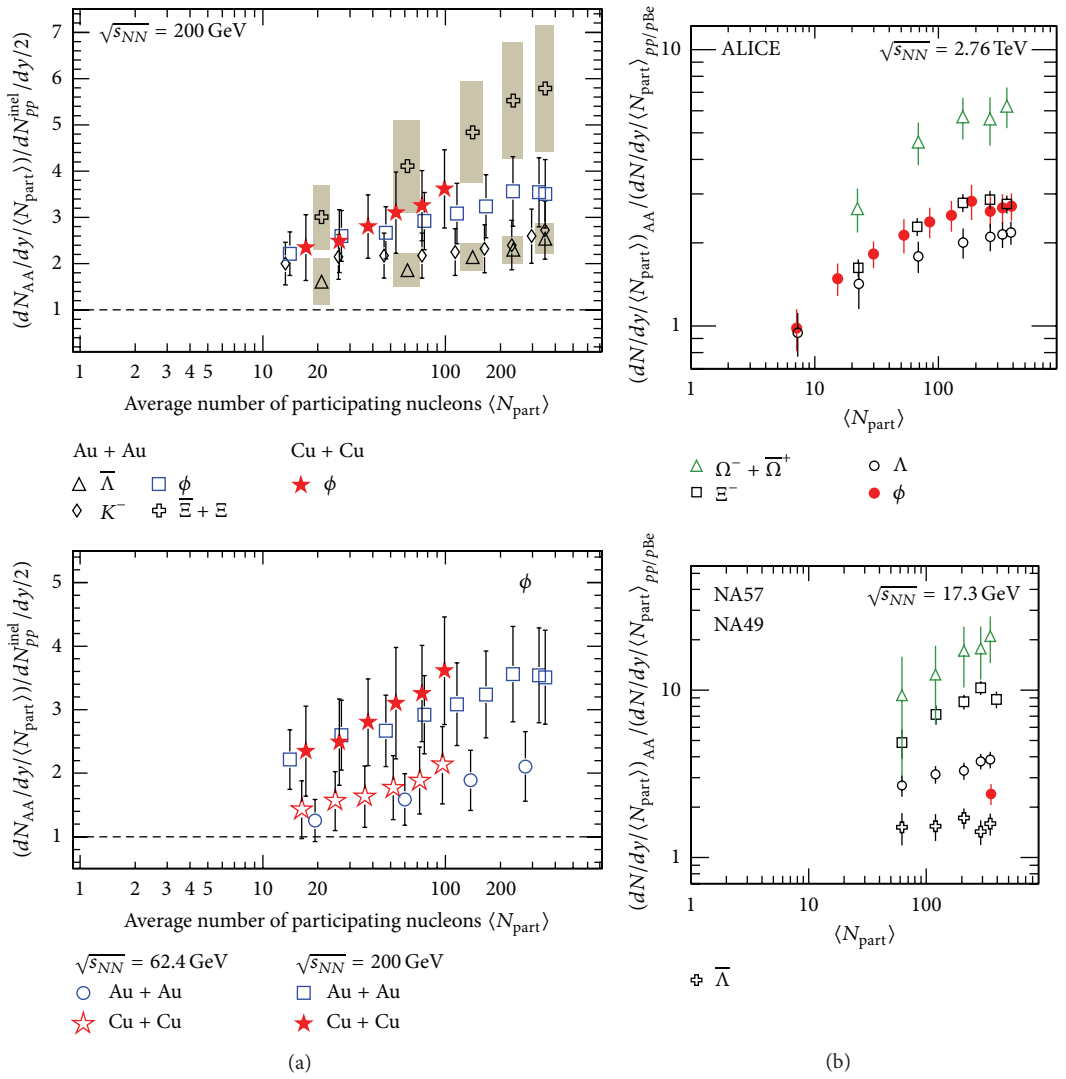

FIGURE 4: (a) The ratio of the yields of K^-, ϕ, $\overline{\Lambda}$, and $\Xi + \overline{\Xi}$ normalised to $\langle N_{part}\rangle$ nucleus-nucleus collisions and to corresponding yields in proton-proton collisions as a function of $\langle N_{part}\rangle$ at 62.4 and 200 GeV [24]. Error bars are quadrature sum of statistical and systematic uncertainties. (b) The ratio of $\langle N_{part}\rangle$ normalised yield of ϕ, Λ, $\overline{\Lambda}$, Ξ^-, and $\Omega^- + \overline{\Omega}^+$ in Pb + Pb collisions to the corresponding yield in $p + p$ (p + Be) collisions at 17.3 GeV (NA57 & NA49) [25, 26] and 2.76 TeV (ALICE) [21]. Only statistical uncertainties are shown.

formation of a dense partonic medium being responsible for the strangeness enhancement in Au + Au collisions at 200 GeV. Furthermore, ϕ mesons do not follow the strange quark ordering as expected in the Canonical picture for the production of other strange hadrons. The observed enhancement in ϕ meson production being related to medium density is further supported by the energy dependence shown in the lower panel of Figure 4. The ϕ meson production relative to $p + p$ collisions is larger at higher beam energy, a trend opposite to that predicted in Canonical models for other strange hadrons.

The right upper panel of Figure 4 shows the enhancement in Pb + Pb with respect to $p + p$ reference yields for ϕ, Λ, Ξ^-, and $\Omega^- + \overline{\Omega}^+$ at $\sqrt{s_{NN}} = 2.76$ TeV [21]. The ϕ, Ξ, and Ω yield in $p + p$ collisions at $\sqrt{s} = 2.76$ TeV have been estimated by interpolating between the measured yields at $\sqrt{s} = 0.9$ TeV and $\sqrt{s} = 7$ TeV. The reference Λ yield in $p + p$ collisions at $\sqrt{s_{NN}} = 2.76$ TeV is estimated by extrapolating from the measured yield in (inelastic) $p + p$ collisions available up to $\sqrt{s} = 0.9$ TeV. Details can be found in [21]. Enhancement factor increases linearly with N_{part} until $N_{part} \approx 100$; then the enhancement values seem to be saturated for higher values of N_{part}. Unlike SPS and RHIC, the order of ϕ enhancement is the same as Ξ^- at LHC energy. We have observed that the ϕ enhancement at central collisions increases from SPS to RHIC energy but the enhancement factor is comparable, within errors, to the values at RHIC and LHC.

These findings tell us that the observed ϕ meson enhancement is not due to the Canonical suppression effects. Therefore this enhancement is very likely due to the formation of a deconfined medium. Since other strange hadrons also emerge from the same system, their enhancement is most likely also

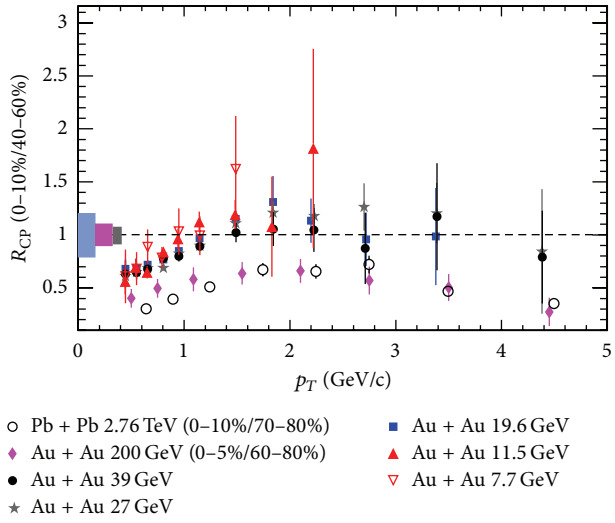

FIGURE 5: The ϕ meson R_{CP} as a function of p_T in Au + Au [17, 18] and Pb + Pb [21] collisions at various beam energies. Error bars are only statistical uncertainties. Bands represent normalisation error from N_{bin} which is approximately 20% for $\sqrt{s_{NN}}$ = 7.7–39 GeV, ~10% for 200 GeV, and ~7% for 2.76 TeV.

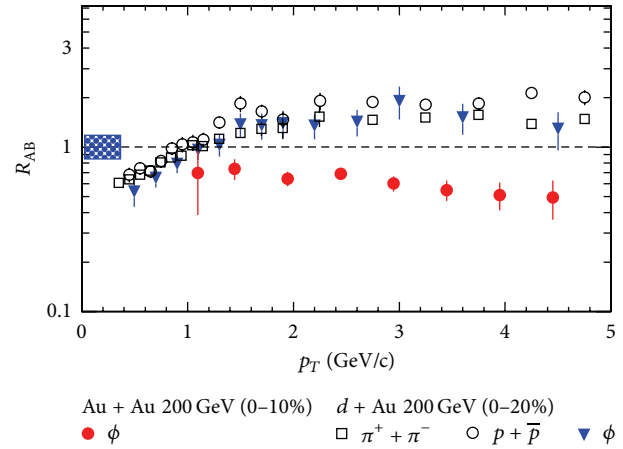

FIGURE 6: The nuclear modification factor R_{AB} as a function of p_T in Au + Au and d + Au [18, 27] collisions at $\sqrt{s_{NN}}$ = 200 GeV. Rectangular bands show the uncertainties associated with estimation of number of binary collisions. Error bars are quadrature sum of statistical and systematic uncertainties for ϕ in d + Au and only statistical for three other cases.

due to formation of deconfined matter or quark-gluon plasma (QGP) in heavy-ion collisions.

2.4. Nuclear Modification Factor. In order to understand parton energy loss in the medium created in high energy heavy-ion collisions for different centralities in A + A collisions, the nuclear modification factor (R_{CP}) is measured which is defined as follows:

$$R_{CP} = \frac{\text{Yield}_{\text{central}}}{\text{Yield}_{\text{peripheral}}} \times \frac{\langle N_{\text{bin}} \rangle_{\text{peripheral}}}{\langle N_{\text{bin}} \rangle_{\text{central}}}, \quad (3)$$

where $\langle N_{\text{bin}} \rangle$ is the average number of binary collisions for the corresponding centrality. The value of N_{bin} was calculated from the Monte Carlo Glauber simulation [43]. R_{CP} value is equal to one when the nucleus-nucleus collisions are simply the superposition of nucleon-nucleon collisions. Therefore deviation of R_{CP} from the unity would imply contribution from the nuclear medium effects, specifically jet-quenching [44]. Nuclear modification factors (R_{CP}) of ϕ mesons at midrapidity in Au + Au collisions at $\sqrt{s_{NN}}$ = 7.7, 11.5, 19.6, 27, 39, and 200 GeV [17, 18] and in Pb + Pb collisions at $\sqrt{s_{NN}}$ = 2.76 TeV [21] are shown in Figure 5. We can see that the R_{CP} of ϕ mesons goes below unity at 200 GeV and 2.76 TeV in nucleus-nucleus collisions. The most feasible explanation of this observation to date is due to the energy loss of the partons traversing the high density QCD medium. This implies that a deconfined medium of quarks and gluons was formed at 200 GeV and 2.76 TeV [18, 21]. For $\sqrt{s_{NN}} \leq$ 39 GeV, ϕ meson R_{CP} is greater than or equal to unity at the intermediate p_T, which indicates that at low energy the parton energy loss contribution to R_{CP} measurement could be less important. In order to confirm that the $R_{CP} < 1$ is due to parton energy loss or jet-quenching phenomenon, it is important to study R_{CP} in p + A or d + A collisions. Nuclear modifications in such systems are expected to be effected by the Cronin effect [45] and not by QGP effect. Due to the Cronin effect the value of R_{CP} at high p_T is expected to be greater than one.

Figure 6 presents the p_T dependence of the nuclear modification factor R_{AB} in Au + Au and d + Au collisions at $\sqrt{s_{NN}}$ = 200 GeV [18, 27]. The definition of R_{AB} is the ratio of the yields of the hadron produced in the nucleus (A) + nucleus (B) collisions to the corresponding yields in the inelastic p + p collisions normalised by N_{bin}. The R_{AB} of ϕ mesons for d + Au collisions show a similar enhancement trend as those for $\pi^+ + \pi^-$ and $p + \overline{p}$ at the intermediate p_T. This enhancement in d + Au collisions was attributed to be due to the Cronin effect [45]. The Cronin enhancement may result either from momentum broadening due to multiple soft [46] (or semihard [47, 48]) scattering in the initial state or from final state interactions as suggested in the recombination model. These mechanisms lead to different particle type and/or mass dependence in the nuclear modification factors as a function of p_T. Current experimental measurements on ϕ meson R_{AB} in d + Au do not seem to have the precision to differentiate between particle type dependence types [49, 50]. On the other hand, the R_{AB} in Au + Au (i.e., R_{AA}) at 200 GeV is lower than that in d + Au at 200 GeV and is less than unity [27]. These features are consistent with the scenario of energy loss of the partons in a QGP medium formed in central Au + Au collisions.

2.5. Mean Transverse Mass. Figure 7 shows the difference in mean transverse mass ($m_T = \sqrt{p_T^2 + m_0^2}$) and rest mass ($m_0$), that is, $\langle m_T \rangle - m_0$ for ϕ meson, as a function of centre-of-mass energy for p + p [18, 20, 22], Au + Au [17, 18], and Pb + Pb [16, 21] collisions. Due to limited statistics, result for p + p at $\sqrt{s}$ = 900 GeV is not shown. The data points in Figure 7 are

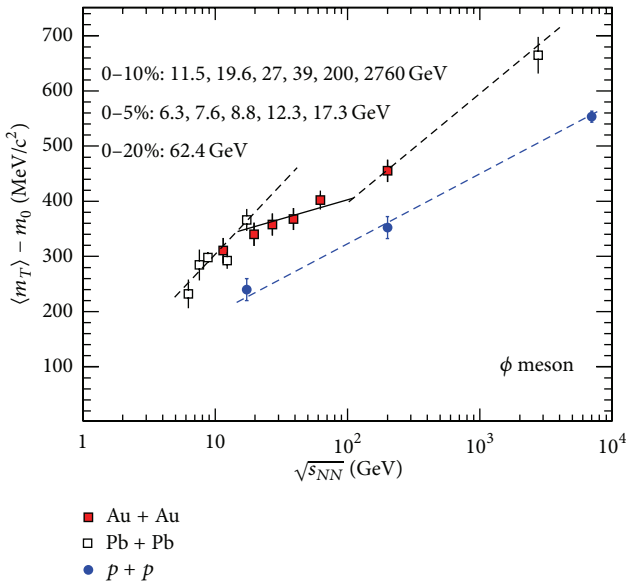

FIGURE 7: $\langle m_T \rangle - m_0$ as a function centre-of-mass energies in central A + A and $p + p$ collisions. Only statistical errors are shown. The dashed and solid lines are the straight lines connected to the data to guide the eye of the reader.

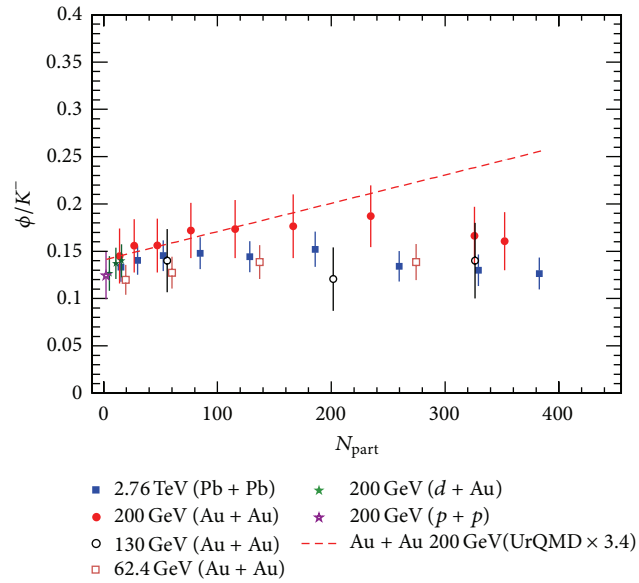

FIGURE 8: ϕ/K^- ratio as a function of number of participants in Au + Au [18] and Pb + Pb [21] collision at various beam energies.

connected by the lines to guide the eye of the reader. One can see that $\langle m_T \rangle - m_0$ increases monotonically with $\sqrt{s_{NN}}$ in $p+p$ collisions whereas the corresponding data in A + A collisions changes slope twice as a function of center-of-mass energy. In A + A collisions, $\langle m_T \rangle - m_0$ first increases with $\sqrt{s_{NN}}$ and then stays independent of energy from approximately 17 GeV to 39 GeV, followed by again an increase with $\sqrt{s_{NN}}$. For a thermodynamic system, the $\langle m_T \rangle - m_0$ can be interpreted as a measure of temperature of the system, and $dN/dy \propto \ln(\sqrt{s_{NN}})$ may represent its entropy. In such a scenario, this observation could reflect the characteristic signature of a first order phase transition [51]. Then the constant value of $\langle m_T \rangle - m_0$ for ϕ meson from 17 GeV to 39 GeV could be interpreted as a formation of a mixed phase of a QGP and hadrons during the evolution of the heavy-ion system.

2.6. Particle Ratios

2.6.1. ϕ/K^-. The mechanism for ϕ meson production in high energy collisions has remained an open issue. In an environment with many strange quarks, ϕ mesons can be produced readily through coalescence, bypassing the OZI rule [52]. On the other hand, a naive interpretation of ϕ meson production in heavy-ion collisions would be the ϕ production via kaon coalescence. In the latter case one could expect an increasing trend of ϕ/K ratio as function of collision centrality and centre-of-mass energy. Models that include hadronic rescatterings such as UrQMD [53, 54] have predicted an increase of the ϕ/K^- ratio at midrapidity as a function of centrality [18]. Therefore, the ratio of ϕ meson yield to that of the kaons can be used to shed light on ϕ meson production mechanism. Figure 8 shows the ϕ/K^- ratio as a function of number of participants for different centre-of-mass energies [18]. The UrQMD model prediction for ϕ/K^- in Au + Au 200 GeV collisions is shown by red dashed line. However, this prediction was disproved from experimental data. It is clear from Figure 8 that ϕ/K^- is independent of centrality and also centre-of-mass energy. In addition, if ϕ production is dominantly from $K\overline{K}$ coalescence, one expects the width of the rapidity distribution of ϕ mesons to be related to those for charged kaons as $1/\sigma^2_\phi = 1/\sigma^2_{K^-} + 1/\sigma^2_{K^+}$. Measurements at SPS energies show a clear deviation of the data from the above expectation [55]. Finally, if ϕ production is dominantly from $K\overline{K}$ coalescence it would be reflected in elliptic flow (v_2) measurements. We observe at intermediate p_T that the v_2 of ϕ mesons and kaons are comparable (discussed in Section 3). All these measurements effectively rule out kaon coalescence as the dominant production mechanism for the ϕ meson for this energy region.

2.6.2. Ω/ϕ. The production mechanism of multistrange hadrons (e.g., ϕ and Ω) is predicted to be very sensitive to the early phase of nuclear collisions [56], because both ϕ and Ω freeze out early, have low hadronic interaction cross-section, and are purely made of strange and antistrange quarks. Therefore the ratio $N(\Omega)/N(\phi)$ is expected to reflect the information of strange quark dynamics in the early stage of the system created in the nucleus-nucleus collision [57]. Figure 9 shows the baryon-to-meson ratio in strangeness sector, $N(\Omega^- + \overline{\Omega}^+)/2N(\phi)$, as a function of p_T in Au + Au collisions at $\sqrt{s_{NN}} = 11.5$ GeV to 2760 GeV [17, 18, 21]. The dashed lines are the results from the recombination model calculation by Hwa and Yang for $\sqrt{s_{NN}} = 200$ GeV [57]. In this model the ϕ and Ω yields in the measured p_T region are mostly from the recombination of thermal strange quarks, which were assumed to follow an exponential p_T distribution.

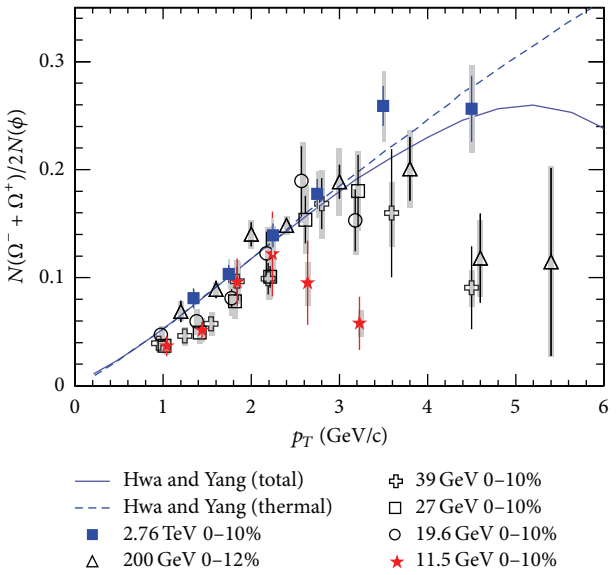

FIGURE 9: The baryon-to-meson ratio, $N(\Omega^- + \overline{\Omega}^+)/2N(\phi)$, as a function of p_T in midrapidity ($|y| < 0.5$) from central A + A collisions at $\sqrt{s_{NN}}$ = 11.5, 19.6, 27, 39, 200, and 2760 GeV [17, 18, 21]. Gray bands denote systematical errors.

The thermal s quark distribution was determined by fitting the low p_T data of kaon production. The contribution from hard parton scattering was assumed to be negligible unless p_T is large. Details of this recombination model have been given in [57]. We can see from Figure 9 that, in central A + A collisions at $\sqrt{s_{NN}} \geq 19.6$ GeV, the ratios of $N(\Omega^- + \overline{\Omega}^+)/2N(\phi)$ in the intermediate p_T range are explained by the recombination model with thermal strange quarks and show a similar trend. The model agrees well with the trend of the data up to $p_T \sim 4$ GeV/c which covers ~95% of the total yields for the ϕ and Ω. The observations imply that the production of ϕ and Ω in central Au + Au collisions is predominantly through the recombination of thermal s quarks for $\sqrt{s_{NN}} \geq 19.6$ GeV. But at $\sqrt{s_{NN}} = 11.5$ GeV, the ratio at the highest measured p_T shows a deviation from the trend of other energies. This may indicate a change in Ω and/or ϕ production mechanism at $\sqrt{s_{NN}} = 11.5$ GeV.

3. Azimuthal Anisotropy in ϕ Meson Production

In noncentral nucleus-nucleus collisions, the initial spatial anisotropy is transformed into a final state momentum anisotropy in the produced particle distributions because of pressure gradient developed due to the interactions among the systems constituents [58–62]. The elliptic flow (v_2) [63–65] is a measure of the second order azimuthal anisotropy of the produced particles in the momentum space. It can be used as probe for the properties of the medium created in the heavy-ion collisions. Because of its self-quenching nature, it carries information from the early phase. Although elliptic flow is an early time phenomenon, its magnitude might still be affected by the later stage hadronic interactions. Since the hadronic interaction cross-section of ϕ meson is smaller than the other hadrons [6] and freezes out relatively early [8], its v_2 remain almost unaffected by the later stage interaction. Therefore ϕ meson v_2 can be considered as good and clean probe for early system created in nucleus-nucleus collisions. Further the ϕ mesons seem to be formed by coalescence of strange quarks and antiquarks in a deconfined medium of quarks and gluons; hence the measurement of collectivity in ϕ mesons would reflect the collectivity in the partonic phase. In addition, its mass is comparable to the masses of the lightest baryon (p and Λ); therefore comparison of ϕ meson v_2 with that of proton and Λ will be helpful to distinguish the mass effect and/or baryon-meson effect in $v_2(p_T)$.

3.1. Differential ϕ Meson v_2. Elliptic flow of ϕ meson as a function of p_T measured at midrapidity [28–31] is shown in Figure 10. The shape of ϕ $v_2(p_T)$ is similar for $\sqrt{s_{NN}}$ = 19.6 GeV to 2760 GeV. But at 7.7 and 11.5 GeV, the ϕ v_2 values at the highest measured p_T bins are observed to be smaller than other energies. Various model studies predicted that ϕ meson v_2 will be small for a system with hadronic interactions [66, 67]. Small interaction cross-section of ϕ meson in hadronic phase suggests that ϕ meson v_2 mostly reflects collectivity from the partonic phase; hence small ϕ meson v_2 indicates less contribution to the collectivity from partonic phase. So the large ϕ meson v_2 at $\sqrt{s_{NN}} \geq$ 15 GeV indicates the formation of partonic matter and small v_2 at $\sqrt{s_{NN}} \leq 11.5$ could indicate dominance of hadron interactions.

3.2. Number-of-Constituent Quark Scaling. In Figure 11, the v_2 scaled by number-of-constituent quarks (n_q) as a function $(m_T - m_0)/n_q$ for identified hadrons in Au + Au collisions at $\sqrt{s_{NN}}$ = 7.7–200 GeV are presented. We can see from Figure 11 that for $\sqrt{s_{NN}}$ = 19.6–200 GeV the v_2 values follow a universal scaling for all the measured hadrons. This observation is known as the NCQ scaling. The observed NCQ scaling at RHIC can be explained by considering particle production mechanism via the quark recombination model and can be considered as a good signature of partonic collectivity [36, 37]. Therefore, such a scaling should vanish for a purely hadronic system if formed in the heavy-ion collisions at the lower energies. At the same time the study of NCQ scaling of identified hadrons from UrQMD model shows that the pure hadronic medium can also reproduce such scaling in v_2 [68–70]. This is due to modification of initially developed v_2 by later stage hadronic interactions and the production mechanism as implemented in the model [69]. Hence to avoid these ambiguities, the v_2 of those particles which do not interact with hadronic interaction will be the clean and good probe for early dynamics in heavy-ion collisions. Due to small hadronic interaction cross-section, ϕ mesons v_2 are almost unaffected by later stage interaction and it will have negligible value if ϕ mesons are not produced via s and $\bar{s}$ quark coalescence [66, 67]. Therefore, NCQ scaling of ϕ mesons v_2 can be considered as the key observables for the partonic collectivity in heavy-ion collisions. As we can see from Figure 11, at $\sqrt{s_{NN}}$ = 7.7 and 11.5 GeV, the ϕ meson v_2

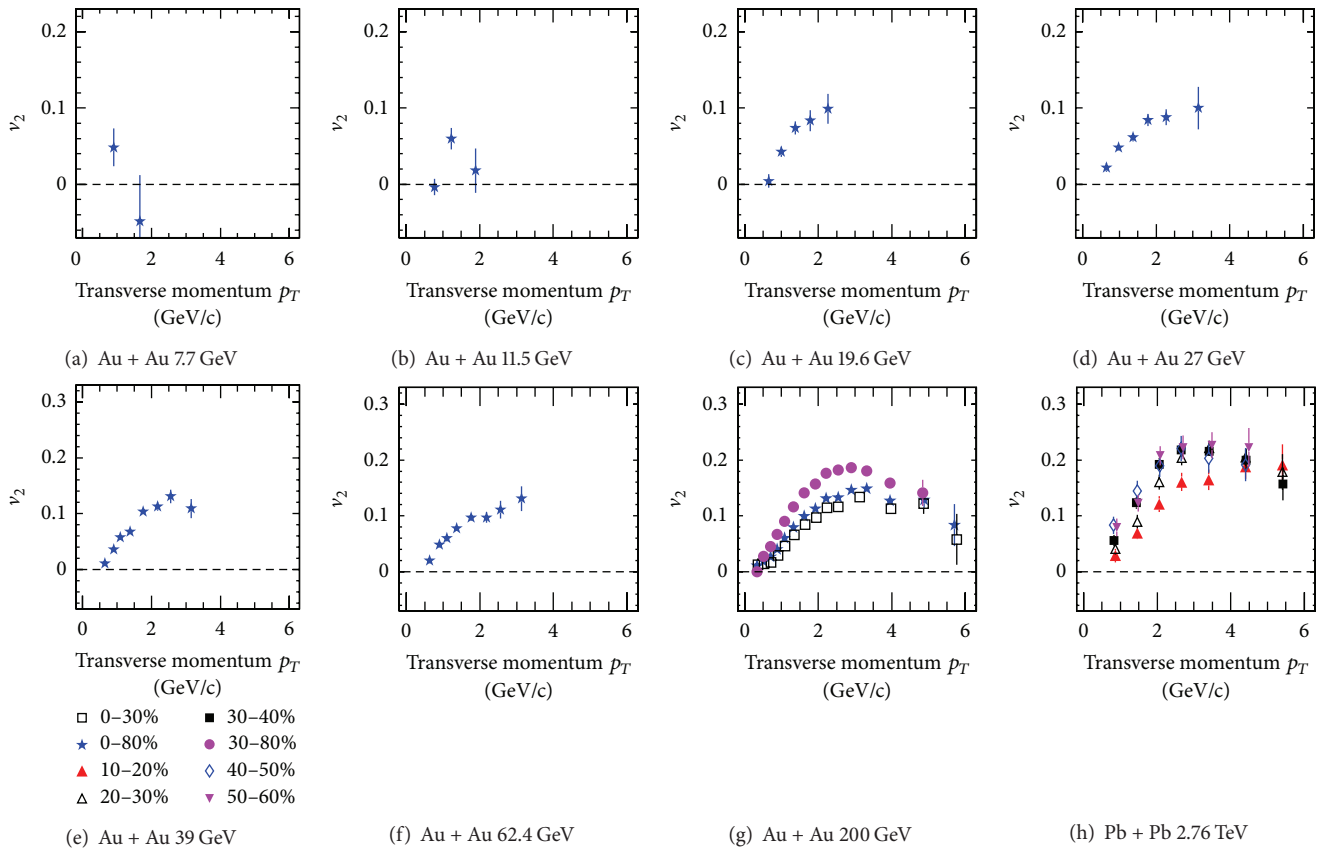

FIGURE 10: The ϕ meson $v_2(p_T)$ at midrapidity in Au+Au collisions at $\sqrt{s_{NN}}$ = 7.7–62.4 GeV for 0–80% centrality [28] and at $\sqrt{s_{NN}}$ = 200 GeV for 0–80%, 0–30%, and 30–80% centralities [29, 30] and in Pb + Pb collisions at $\sqrt{s_{NN}}$ = 2.76 TeV [31] for different collisions centralities. The vertical lines are statistical uncertainties.

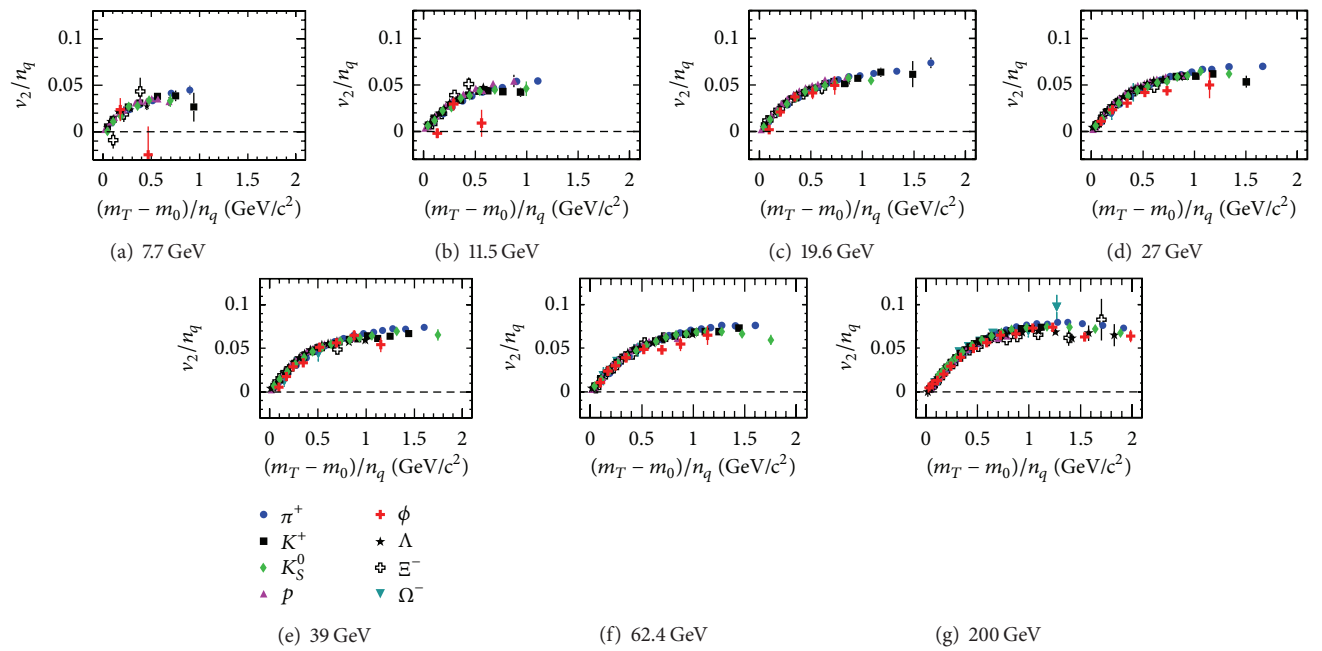

FIGURE 11: The NCQ-scaled elliptic flow, v_2/n_q, versus $(m_T - m_0)/n_q$ for 0–80% central Au + Au collisions for selected identified particles [28–30]. Only statistical error bars are shown.

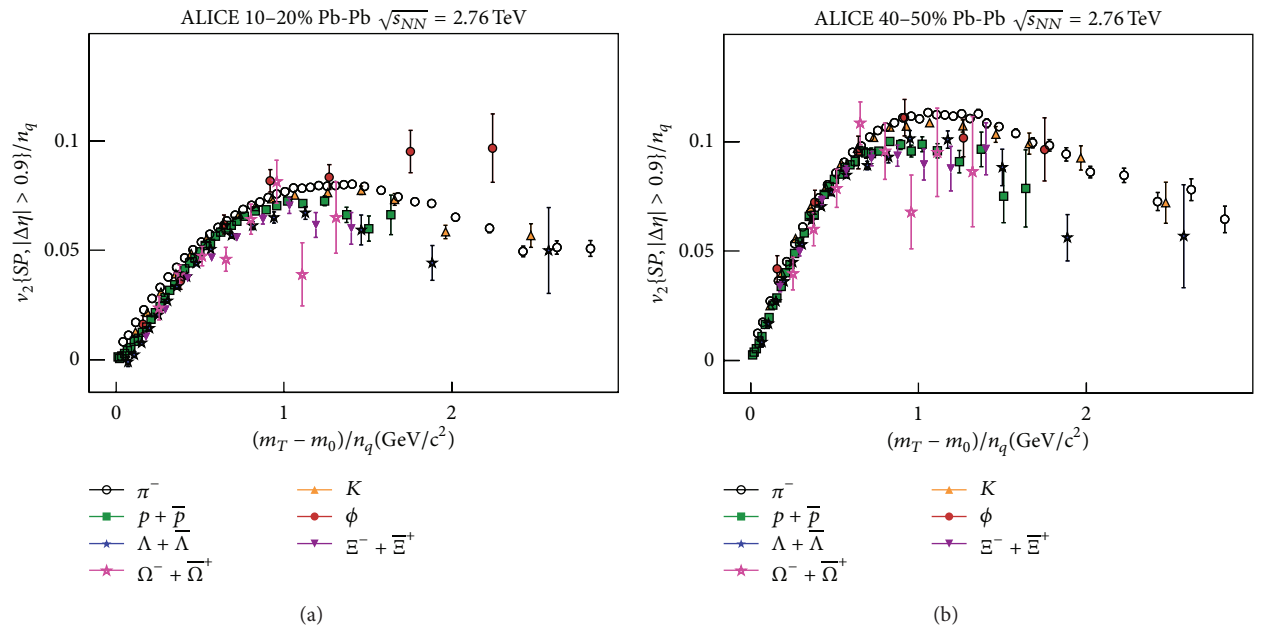

FIGURE 12: The NCQ-scaled elliptic flow, v_2/n_q, versus $(m_T - m_0)/n_q$ for 10–20% and 40–50% central Pb + Pb collisions for selected identified particles [31]. Only statistical error bars are shown. The figure has been taken from the presentation at Quark Matter 2014 by ALICE collaboration.

deviates from the trend of the other hadrons at the highest measured p_T values by 1.8σ and 2.3σ, respectively. This could be the effect for a system, where hadronic interactions are more important.

Figure 12 presents the $(m_T - m_0)/n_q$ dependence of v_2/n_q for 10–20% and 40–50% central Pb + Pb collisions for selected identified particles [31]. It can be seen that, at higher value of $(m_T - m_0)/n_q$, the scaling is not good compared to that observed at RHIC energies. There are deviations at the level of ±20% with respect to the reference ratio as shown in [31]. This larger deviation at LHC energy could be related to observed large radial flow at LHC compared to RHIC.

3.3. p_T Integrated ϕ Meson v_2. The p_T integrated elliptic flow ($\langle v_2 \rangle$) can be calculated as

$$\langle v_2 \rangle = \frac{\int v_2(p_T)(dN/dp_T)\,dp_T}{\int (dN/dp_T)\,dp_T}. \quad (4)$$

Figure 13 shows p_T integrated ϕ meson (red star) and proton (blue circle) v_2 as a function of centre-of-mass energy for 0–80% centrality [32]. One can see that for both particle species the $\langle v_2 \rangle$ increases with increasing beam energy. ϕ meson $\langle v_2 \rangle$ from a multiphase transport (AMPT) model for three different scenarios is shown by shaded bands. Green band corresponds to AMPT default model which includes only hadronic interaction whereas black and yellow bands correspond to AMPT with string melting scenario with parton-parton cross-sections of 3 mb and 10 mb, respectively. In contrast to observations from the data, the $\langle v_2 \rangle$ values from model remain constant for all the energies. This is because they have been obtained for a fixed parton-parton interaction cross-section. The $\langle v_2 \rangle$ of ϕ mesons for $\sqrt{s_{NN}} \geq 19.6$ GeV can be explained by the AMPT with string melting (SM) version, by varying the parton-parton cross-section. On the other hand, both the AMPT-SM and the AMPT default models overpredict data at $\sqrt{s_{NN}} = 11.5$ GeV. The comparison to AMPT model results indicates negligible contribution of the partonic interactions to the final measured collectivity for $\sqrt{s_{NN}} = 11.5$ GeV. For $\sqrt{s_{NN}} > 19.6$ GeV, proton and ϕ meson show similar magnitude of $\langle v_2 \rangle$. The proton is a baryon and ϕ is a meson; in addition they are composed of different quark flavours, yet they have similar $\langle v_2 \rangle$; this is a strong indication of large fraction of the collectivity being developed in the partonic phase. However at $\sqrt{s_{NN}} \leq 19.6$ GeV, ϕ meson $\langle v_2 \rangle$ values show deviation from that for proton and at $\sqrt{s_{NN}} = 11.5$ GeV ϕ meson $\langle v_2 \rangle$ becomes small (~1.5%). This tells us that due to the lack of enough partonic interactions at lower beam energies a larger $\langle v_2 \rangle$ could not be generated for ϕ mesons. The contribution to ϕ $\langle v_2 \rangle$ from hadronic interactions is small because of small ϕ-hadron interaction cross-sections. However the observed higher collectivity of protons compared to ϕ mesons at the lower beam energies could be due to the protons having larger hadronic interaction cross-section.

3.4. Hadronic Rescattering Effect on v_2. Recent phenomenological calculation based on ideal hydrodynamical model together with the later stage hadron cascade (hydro + JAM) shows that the mass ordering of v_2 could be broken between that of ϕ meson and that of proton at low p_T ($p_T < 1.5$ GeV/c) [71]. This is because of late stage hadronic rescattering effects on proton v_2. The model calculation was done by considering low hadronic interaction cross-section for ϕ meson and larger hadronic interaction cross-section for proton. The ratio between ϕ v_2 and proton v_2 is shown in Figure 14 for

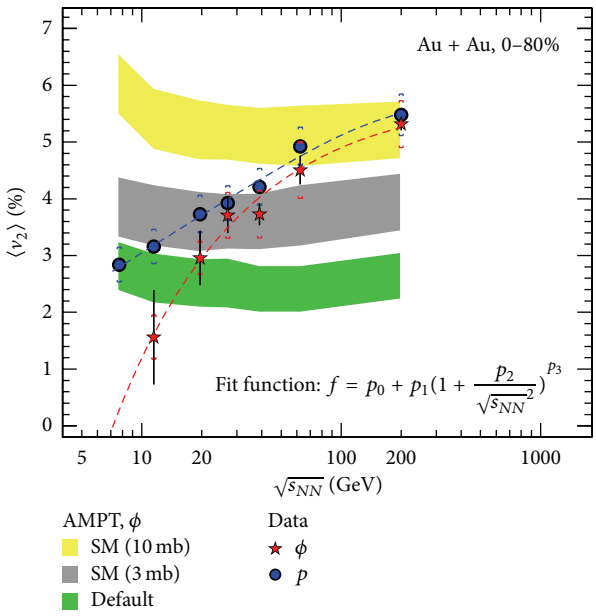

FIGURE 13: The p_T integrated proton and ϕ meson v_2 for various centre-of-mass energies for 0–80% centrality in Au + Au collisions [32]. Vertical lines are the statistical error and systematic errors are shown by cap symbol. For lower RHIC energies, STAR preliminary p_T spectra were used for ϕ and proton $\langle v_2 \rangle$ calculation [17, 33, 34]. The red and blue lines are the fit to the ϕ and proton v_2 by empirical function just to guide the eye of the reader.

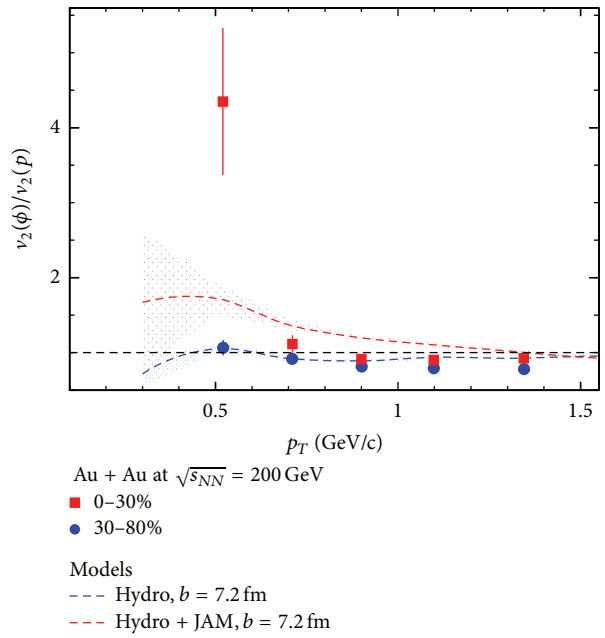

FIGURE 14: Ratio between ϕ and p v_2 for 0–30% and 30–80% centrality in Au + Au collisions $\sqrt{s_{NN}}$ = 200 GeV [29, 30].

minimum bias Au + Au collisions at $\sqrt{s_{NN}}$ = 200 GeV. The data from the STAR experiment are shown by solid red square and blue solid circle [29, 30]. Solid red square and blue solid circle correspond to 0–30% and 30–80% centralities, respectively. The ratios are larger than unity at low p_T region ($p_T < 0.7$ GeV/c) for 0–30% centrality although mass of the ϕ meson (1.019 GeV/c^2) is greater than mass of the proton (0.938 GeV/c^2). This is qualitatively consistent with the model calculation using hydro + JAM shown by red bands. Therefore this observation is consistent with the physical scenario of larger effect of hadronic rescattering on proton v_2 which reduces its value, as predicted in the theoretical model [67, 71]. Due to small hadronic interaction cross-section ϕ meson v_2 remains unaffected by later stage hadronic rescattering.

4. Summary

We have presented a review on the experimentally measured data on ϕ production (specifically the transverse momentum distributions and azimuthal anisotropy measurements) in high energy heavy-ion collisions. The differential (p_T, φ, y) measurements of ϕ meson production have been compared from heavy-ion collisions at the SPS, RHIC, and LHC energies. Transverse momentum spectra of ϕ meson for different centralities, different energies, and different collision systems are presented. The shape of the transverse momentum distribution changes from exponential to Levy functional form as one goes from central to peripheral collisions at a given beam energy. This indicates an increasing contribution of hard processes in the peripheral collisions. The centrality and energy dependence of the enhancement in ϕ meson production support the physical origin to be due to the enhanced production of $s(\bar{s})$-quarks in a dense partonic medium formed in high energy heavy-ion collisions. We have discussed beam energy dependence of the nuclear modification factors of ϕ meson. The values of nuclear modification factors are less than unity for beam energies of 200 GeV and 2.76 TeV, indicating formation of a dense medium with color degrees of freedom. The nuclear modification factor values at the intermediate p_T are observed to be equal to or higher than unity at $\sqrt{s_{NN}} \leq 39$ GeV. This indicates that parton energy loss effect became less important and suggests dominance of hadronic interactions at the lower beam energies. The ratio $N(\phi)/N(K^-)$ is observed to be almost constant as a function of centrality and centre-of-mass energy, disfavouring ϕ meson production through kaon coalescence. The ratio of $N(\Omega^- + \overline{\Omega}^+)/2N(\phi)$ versus p_T shows a similar trend for $\sqrt{s_{NN}} \geq 19.6$ GeV, but at $\sqrt{s_{NN}} = 11.5$ GeV the ratio at the highest measured p_T shows a deviation from the trend at other higher energies. This may suggest a change in Ω and/or ϕ production mechanism and strange quark dynamics in general at $\sqrt{s_{NN}} = 11.5$ GeV.

The measurement of ϕ meson v_2 as a function of p_T and collision centrality are discussed. We observe that ϕ meson $v_2(p_T)$ has similar values for $\sqrt{s_{NN}} \geq 19.6$ GeV and NCQ scaling also holds for $\sqrt{s_{NN}} \geq 19.6$ GeV. But at $\sqrt{s_{NN}} = 7.7$ and 11.5 GeV, the ϕ meson v_2 shows deviation from the other hadrons at the highest measured p_T values by 1.8σ and 2.3σ, respectively. Since the v_2 of ϕ mesons mostly reflect collectivity from partonic phase, therefore the small ϕ v_2 observed at $\sqrt{s_{NN}} = 7.7$ and 11.5 GeV indicates a smaller contribution to the collectivity from partonic phase. We

find that the ϕ $\langle v_2 \rangle$ can be explained by AMPT model with partonic interactions having cross-section values between 3 mb and 10 mb for $\sqrt{s_{NN}} \geq 19.6$ GeV, but the model with and without partonic interactions overpredicts the data at $\sqrt{s_{NN}} = 7.7$ and 11.5 GeV. Also at $\sqrt{s_{NN}} > 19.6$ GeV, proton and ϕ meson show similar magnitude of $\langle v_2 \rangle$; however, at $\sqrt{s_{NN}} \leq 19.6$ GeV, ϕ meson $\langle v_2 \rangle$ shows deviation from corresponding proton values. At $\sqrt{s_{NN}} = 11.5$ GeV ϕ meson $\langle v_2 \rangle$ value is small and is about 1.5%. This further emphasises our conclusion that at lower beam energies the hadronic interactions are dominating. In addition, we observe that the mass ordering between ϕ and proton v_2 breaks down in the lower momentum range at $\sqrt{s_{NN}} = 200$ GeV. This could be because of the larger effect of hadronic rescattering on proton v_2, which reduces the proton v_2 values.

The main conclusions of the review are the following. (a) The coalescence of K^+ and K^- is not the dominant production mechanism for ϕ meson in high energy heavy-ion collisions. (b) The study of Ω/ϕ and comparison to quark recombination model calculations indicate that ϕ mesons are produced via coalescence of thermalized s quarks for $\sqrt{s_{NN}} \geq 19.6$ GeV. (c) The observed ϕ meson enhancement (unaffected by Canonical suppression effects) in heavy-ion collisions suggests that strangeness enhancement is due to the formation of a dense partonic medium. (d) The nuclear modification factor measurements for ϕ mesons and the measurements of ϕ meson v_2 indicate the formation of partonic media in heavy-ion collisions at $\sqrt{s_{NN}} \geq 19.6$ GeV, while for $\sqrt{s_{NN}} \leq 11.5$ GeV hadronic interactions dominate. (e) Finally ϕ meson production provided us with a benchmark to study the rescattering effect. The comparison of ϕ and proton v_2 shows that mass ordering in $v_2(p_T)$ could be broken due to effect of later stage rescattering effects on the proton distributions.

Conflict of Interests

The authors declare that there is no conflict of interests regarding the publication of this paper.

Acknowledgments

Financial assistance from the SwarnaJayanti Fellowship of the Department of Science and Technology. Government of India, is gratefully acknowledged. Md. Nasim is supported by DOE Grant of Department of Physics and Astronomy, UCLA, USA.

References

[1] F. Karsch, "Lattice results on QCD thermodynamics," *Nuclear Physics A*, vol. 698, no. 1–4, pp. 199–208, 2002.

[2] R. V. Gavai and S. Gupta, "On the critical end point of QCD," *Physical Review D*, vol. 71, no. 11, Article ID 114014, 21 pages, 2005.

[3] K. G. Wilson, "Confinement of quarks," *Physical Review D*, vol. 10, p. 2445, 1974.

[4] S. Bethke, "Experimental tests of asymptotic freedom," *Progress in Particle and Nuclear Physics*, vol. 58, no. 2, pp. 351–386, 2007.

[5] L. Bertanza, V. Brisson, P. L. Connolly et al., "Possible Resonances in the $\Xi\pi$ and $K\overline{K}$ Systems," *Physical Review Letters*, vol. 9, no. 4, pp. 180–183, 1962.

[6] A. Shor, "φ-meson production as a probe of the Quark-Gluon plasma," *Physical Review Letters*, vol. 54, no. 11, pp. 1122–1125, 1985.

[7] A. Sibirtsev, H.-W. Hammer, U.-G. Meißner, and A. W. Thomas, "φ-meson photoproduction from nuclei," *The European Physical Journal*, vol. 29, no. 2, pp. 209–220, 2006.

[8] J. Adams, M. M. Aggarwal, Z. Ahammed et al., "Experimental and theoretical challenges in the search for the quark-gluon plasma: The STAR Collaboration's critical assessment of the evidence from RHIC collisions," *Nuclear Physics A*, vol. 757, no. 1-2, pp. 102–183, 2005.

[9] P. Koch, B. Müllerb, and J. Rafelskic, "Strangeness in relativistic heavy ion collisions," *Physics Reports*, vol. 142, no. 4, pp. 167–262, 1986.

[10] T. Alber, H. Appelshäuser, J. Bächler et al., "Strange particle production in nuclear collisions at 200 GeV per nucleon," *Zeitschrift für Physik C*, vol. 64, no. 2, pp. 195–207, 1994.

[11] P. G. Jones, "Hadron yields and hadron spectra from the NA49 experiment," *Nuclear Physics A*, vol. 610, p. 188c, 1996.

[12] F. Siklér, J. Bächlerf, D. Barna et al., "Hadron production in nuclear collisions from the NA49 experiment at 158 GeV/c. A," *Nuclear Physics A*, vol. 611, no. 1–4, pp. 45–54, 1996.

[13] C. Hohne, "Strangeness production in nuclear collisions—recent results from experiment NA49," *Nuclear Physics A*, vol. 611, pp. 485–488, 1999.

[14] J. Rafelski and B. Müller, "Strangeness production in the quark-gluon plasma," *Physical Review Letters*, vol. 48, no. 16, pp. 1066–1069, 1982.

[15] K. Redlich and A. Tounsi, "Strangeness enhancement and energy dependence in heavy ion collisions," *European Physical Journal C*, vol. 24, no. 4, pp. 589–594, 2002.

[16] C. Alt, T. Anticic, B. Baatar et al., "Energy dependence of ϕ meson production in central Pb+Pb collisions at $\sqrt{s_{NN}} = 6$ to 17 GeV," *Physical Review C*, vol. 78, no. 4, 15 pages, 2008.

[17] M. Nasim, "Probing the QCD phase diagram with measurements of ϕ-meson production and elliptic flow in heavy-ion collisions at STAR," *Journal of Physics: Conference Series*, vol. 509, no. 1, Article ID 10.1088/1742-6596/509/1/012070, 2014.

[18] B. I. Abelev et al., "Measurements of ϕ meson production in relativistic heavy-ion collisions at the BNL Relativistic Heavy Ion Collider (RHIC)," *Physical Review C*, vol. 49, Article ID 064903, 2009.

[19] B. Abelev, A. Abrahantes Quintana, D. Adamová et al., "Strange particle production in proton–proton collisions at $\sqrt{s} = 0.9$ TeV with ALICE at the LHC," *The European Physical Journal C*, vol. 71, p. 1594, 2011.

[20] B. Abelev, J. Adam, D. Adamová et al., "Production of $K^*(892)^\circ$ and $\phi(1020)$ in pp collisions at $\sqrt{s} = 7$ TeV," *The European Physical Journal C*, vol. 72, article 2183, 2012.

[21] B. B. Abelev, J. Adam, D. Adamova et al., "$K^*(892)^0$ and $\Phi(1020)$ production in Pb-Pb collisions at $\sqrt{s_{NN}} = 2.76$ TeV," In press, http://arxiv.org/abs/1404.0495.

[22] S. V. Afanasiev, T. Anticicu, J. Bächler et al., "Production of φ-mesons in $p + p$, $p +$ Pb and central Pb + Pb collisions at $E_{beam} =$ 158 A GeV," *Physics Letters B*, vol. 491, no. 1-2, pp. 59–66, 2000.

[23] T. Akesson, "Inclusive vector-meson production in the central region of pp collisions at $\sqrt{s} = 63$ GeV," *Nuclear Physics B*, vol. 203, no. 1, pp. 27–99, 1982.

[24] B. I. Abelev, M. M. Aggarwal, Z. Ahammed et al., "Energy and system size dependence of ϕ meson production in Cu+Cu and Au+Au collisions," *Physics Letters B*, vol. 673, pp. 183–191, 2009.

[25] F. Antinori, P. Bacon, A. Badalà et al., "Enhancement of hyperon production at central rapidity in 158 *A* GeV/*c* Pb–Pb collisions," *Journal of Physics G*, vol. 32, no. 4, article 427, 2006.

[26] S. V. Afanasev, T. Anticic, J. Bächler et al., "Production of φ-mesons in $p + p$, p + Pb and central Pb + Pb collisions at E_{beam} = 158A GeV," *Physics Letters B*, vol. 491, p. 59, 2000.

[27] A. Adare, S. Afanasiev, C. Aidala et al., "Nuclear modification factors of ϕ mesons in $d + Au$, $Cu + Cu$, and $Au + Au$ collisions at $\sqrt{s_{NN}} = 200$," *Physical Review C*, vol. 83, no. 2, Article ID 024909, 10 pages, 2011.

[28] L. Adamczyk, J. K. Adkins, G. Agakishiev et al., "Elliptic flow of identified hadrons in Au+Au collisions at $\sqrt{s_{NN}}$ = 7.7–62.4 GeV," *Physical Review C*, vol. 88, Article ID 014902, 2013.

[29] M. Nasim and The STAR Collaboration, "Systematic investigation of partonic collectivity through centrality dependence of elliptic flow of multi-strange hadrons in $Au + Au$ collisions at $\sqrt{s_{NN}} = 200$ GeV," *Nuclear Physics A*, vol. 904-905, pp. 413c–416c, 2013.

[30] R. Haque and M. K. Sharma, STAR presentation at QM2014.

[31] B. Abelev, "Elliptic flow of identified hadrons in Pb-Pb collisions at $\sqrt{s_{NN}}$ = 2.76 TeV," http://arxiv.org/abs/1405.4632.

[32] M. Nasim, "Using ϕ-meson elliptic flow to map the strength of the partonic interaction," *Physical Review C*, vol. 89, Article ID 034909, 2014.

[33] L. Kumar, "STAR results from the RHIC beam energy scan-I," *Nuclear Physics A*, vol. 904-905, pp. 256c–263c, 2013.

[34] S. Das and The STAR Collaboration, "Study of freeze-out dynamics in STAR at RHIC beam energy scan program," *Journal of Physics: Conference Series*, vol. 509, conference 1, Article ID 012066, 2014.

[35] J. Adams, C. Adler, M. M. Aggarwal et al., "Particle-type dependence of azimuthal anisotropy and nuclear modification of particle production in Au+Au collisions at $\sqrt{s_{NN}}$ = 200 GeV," *Physical Review Letters*, vol. 92, no. 5, Article ID 052302, 6 pages, 2004.

[36] D. Molnar and S. A. Voloshin, "Elliptic flow at large transverse momenta from quark coalescence," *Physical Review Letters*, vol. 91, no. 9, Article ID 092301, 4 pages, 2003.

[37] R. J. Fries, B. Müller, C. Nonaka, and S. A. Bass, "Hadronization in heavy-ion collisions: recombination and fragmentation of partons," *Physical Review Letters*, vol. 90, no. 20, Article ID 202303, 2003.

[38] G. Aad, T. Abajyan, B. Abbott et al., "The differential production cross section of the ϕ (1020) meson in $\sqrt{s}$ = 7 TeV pp collisions measured with the ATLAS detector," *The European Physical Journal C*, vol. 74, p. 2895, 2014.

[39] V. Khachatryan, A. M. Sirunyan, A. Tumasyan et al., "Transverse-momentum and pseudorapidity distributions of charged hadrons in pp collisions at $\sqrt{s}$ = 7 TeV," *Physical Review Letters*, vol. 105, Article ID 022002, 2010.

[40] S. Chatrchyan, V. Khachatryan, A. M. Sirunyan et al., "Study of the inclusive production of charged pions, kaons, and protons in pp collisions at $\sqrt{s}$ = 0.9, 2.76, and 7 TeV," *The European Physical Journal C*, vol. 72, p. 2164, 2012.

[41] V. Blobel, H. Fesefeldt, H. Franz et al., "Test of the Zweig selection rule in Φ production by pp collisions," *Physics Letters B*, vol. 59, no. 1, pp. 88–92, 1975.

[42] A. Sibirtsev, J. Haidenbauer, and U.-G. Meissner, "Aspects of phi-meson production in proton-proton collisions," *The European Physical Journal A*, vol. 27, no. 3, pp. 263–268, 2006.

[43] M. L. Miller, K. Reygers, S. J. Sanders, and P. Steinberg, "Glauber modeling in high-energy nuclear collisions," *Annual Review of Nuclear and Particle Science*, vol. 57, pp. 205–243, 2007.

[44] X. N. Wang and M. Gyulassy, "Gluon shadowing and jet quenching in A+A collisions at $\sqrt{s}$ =200A GeV," *Physical Review Letters*, vol. 68, no. 10, pp. 1480–1483, 1992.

[45] J. W. Cronin, H. J. Frisch, M. J. Shochet, J. P. Boymond, P. A. Piroué, and R. L. Sumner, "Production of hadrons at large transverse momentum at 200, 300, and 400 GeV," *Physical Review D*, vol. 11, p. 3105, 1975.

[46] M. Lev and B. Petersson, "Nuclear effects at large transverse momentum in a QCD parton model," *Zeitschrift für Physik C Particles and Fields*, vol. 21, no. 1, pp. 155–161, 1983.

[47] A. Accardi and M. Gyulassy, "Cronin effect vs. geometrical shadowing in d + Au collisions at RHIC," *Physics Letters B: Nuclear, Elementary Particle and High-Energy Physics*, vol. 586, no. 3-4, pp. 244–253, 2004.

[48] G. Papp, P. Lévai, and G. Fai, "Saturating Cronin effect in ultrarelativistic proton-nucleus collisions," *Physical Review C*, vol. 61, no. 2, Article ID 021902(R), 5 pages, 1999.

[49] R. C. Hwa, C. B. Yang, and R. J. Fries, "Forward production in d+Au collisions by parton recombination," *Physical Review C*, vol. 71, no. 2, Article ID 024902, 9 pages, 2005.

[50] B. I. Abelev, J. Adams, M. M. Aggarwal et al., "Rapidity and species dependence of particle production at large transverse momentum for d + Au collisions at $\sqrt{s_{NN}}$ = 200 GeV," *Physical Review C*, vol. 76, Article ID 054903, 2007.

[51] L. van Hove, "Multiplicity dependence of p_t spectrum as a possible signal for a phase transition in hadronic collisions," *Physics Letters B*, vol. 118, no. 1–3, pp. 138–140, 1982.

[52] N. Isgur and H. B. Thacker, "Origin of the Okubo-Zweig-Iizuka rule in QCD," *Physical Review D*, vol. 64, no. 9, Article ID 094507, 13 pages, 2001.

[53] S. A. Bass, M. Belkacem, M. Bleicher et al., "Microscopic models for ultrarelativistic heavy ion collisions," *Progress in Particle and Nuclear Physics*, vol. 41, pp. 255–369, 1998.

[54] M. Bleicher, E. Zabrodin, C. Spieles et al., "Relativistic hadron-hadron collisions in the ultra-relativistic quantum molecular dynamics model," *Journal of Physics G: Nuclear and Particle Physics*, vol. 25, no. 9, article 1859, 1999.

[55] C. Alt, T. Anticic, B. Baatar et al., "System-size dependence of strangeness production in nucleus-nucleus collisions at $\sqrt{s_{NN}}$ = 17.3 GeV," *Physical Review Letters*, vol. 94, no. 5, Article ID 052301, 5 pages, 2005.

[56] J. Adams, C. Adler, M. M. Aggarwal et al., "Multistrange Baryon Production in Au-Au Collisions at $\sqrt{s_{NN}}$ = 130 GeV," *Physical Review Letters*, vol. 92, no. 18, Article ID 182301, 6 pages, 2004.

[57] R. C. Hwa and C. B. Yang, "Production of strange particles at intermediate p_T in central Au+Au collisions at high energies," *Physical Review C*, vol. 75, Article ID 054904, p. 054904, 2007.

[58] P. F. Kolb and U. Heinz, "Emission angle dependent HBT at RHIC and beyond," *Nuclear Physics A*, vol. 715, pp. 653c–656c, 2003.

[59] D. Teaney, J. Lauret, and E. V. Shuryak, "Flow at the SPS and RHIC as a quark-gluon plasma signature," *Physical Review Letters*, vol. 86, no. 21, pp. 4783–4786, 2001.

[60] P. F. Kolb and U. Heinz, "Hydrodynamic description of ultrarelativistic heavy-ion collisions," http://arxiv.org/abs/nucl-th/0305084.

[61] P. F. Kolba, P. Huovinend, U. Heinza, and H. Heiselberge, "Elliptic flow at SPS and RHIC: from kinetic transport to hydrodynamics," *Physics Letters B*, vol. 500, no. 3-4, pp. 232–240, 2001.

[62] H. Sorge, "Elliptical flow: a signature for early pressure in ultra-relativistic nucleus-nucleus collisions," *Physical Review Letters*, vol. 78, pp. 2309–2312, 1997.

[63] J. Y. Ollitrault, "Anisotropy as a signature of transverse collective flow," *Physical Review D*, vol. 46, p. 229, 1992.

[64] P. Huovinen, P. F. Kolb, U. Heinz et al., "Radial and elliptic flow at RHIC: further predictions," *Physics Letters B*, vol. 503, pp. 58–64, 2001.

[65] A. M. Poskanzer and S. A. Voloshin, "Methods for analyzing anisotropic flow in relativistic nuclear collisions," *Physical Review C*, vol. 58, no. 3, pp. 1671–1678, 1998.

[66] B. Mohanty and N. Xu, "Probe of the QCD phase diagram with phi-mesons in high-energy nuclear collisions," *Journal of Physics G*, vol. 36, no. 6, Article ID 064022, 2009.

[67] M. Nasim, B. Mohanty, and N. Xu, "Elliptic flow of ϕ mesons as a sensitive probe for the onset of the deconfinement transition in high energy heavy-ion collisions," *Physical Review C*, vol. 87, no. 1, Article ID 014903, 4 pages, 2013.

[68] P. Bhaduri and S. Chattopadhyay, "Differential elliptic flow of identified hadrons and constituent quark number scaling at the GSI Facility for Antiproton and Ion Research (FAIR)," *Physical Review C*, vol. 81, Article ID 034906, 2010.

[69] K. J. Wu, F. Liu, and N. Xu, "The number-of-quark scaling of v2 in $\sqrt{s_{NN}}$ = 9.2 GeV Au+Au collisions," *Nuclear Physics A*, vol. 834, no. 1, pp. 303c–305c, 2010.

[70] M. Bleicher and X. Zhu, "Is constituent quark scaling a unique sign of parton recombination?" *European Physical Journal C*, vol. 49, no. 1, pp. 303–308, 2007.

[71] T. Hirano, U. Heinz, D. Kharzeev, R. Lacey, and Y. Nara, "Mass ordering of differential elliptic flow and its violation for ϕ mesons," *Physical Review C*, vol. 77, Article ID 044909, 2008.